Environmental Science & Technology

ARTICLE

pubs.acs.org/est

Impact of Porous Media Grain Size on the Transport of Multi-walled Carbon Nanotubes

Nikolai T. Mattison,[†] Denis M. O'Carroll,[†,∥,*] R. Kerry Rowe,[‡] and Elijah J. Petersen[§]

[†]Department of Civil & Environmental Engineering, The University of Western Ontario, London, ON, Canada N6A 5B8

[∥]Water Research Laboratory, School of Civil and Environmental Engineering, University of New South Wales, Manly Vale, NSW, 2093, Australia

[‡]GeoEngineering Centre at Queen's-RMC, Queen's University, Kingston, Ontario, Canada K7L 3N6

[§]Material Measurement Laboratory, National Institute of Standards and Technology, Gaithersburg, Maryland 20899, United States

Supporting Information

ABSTRACT: Nanoparticles possess unique physical, electrical, and chemical properties which make them attractive for use in a wide range of consumer products. Through their manufacturing, usage, and eventual disposal, nanoparticles are expected to ultimately be released to the environment after which point they may pose environmental and human health risks. One critical component of understanding and modeling those potential risks is their transport in the subsurface environment. This study investigates the mobility of one important nanoparticle (multi-walled carbon nanotubes or MWCNTs) through porous media, and makes the first measurements on the impact of mean collector grain size (d_{50}) on MWCNT retention. Results from one-dimensional column experiments conducted under various physical and chemical conditions coupled with results of numerical modeling assessed the suitability of traditional transport models to predict MWCNT mobility. Findings suggest that a dual deposition model coupled with site blocking greatly improves model fits compared to traditional colloid filtration theory. Of particular note is that the MWCNTs traveled through porous media ranging in size from fine sand to silt resulting in normalized concentrations of MWCNTs in the effluent in excess of 60% of the influent concentration.

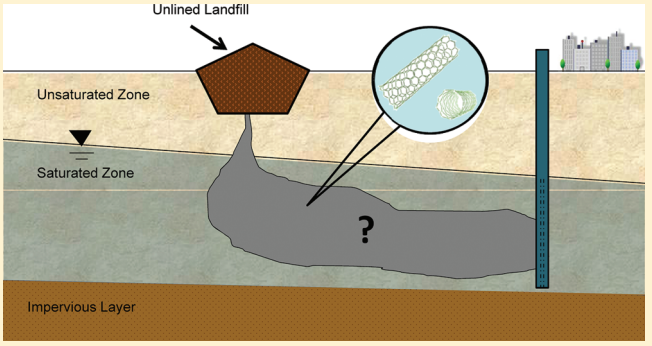

INTRODUCTION

Increased production and utilization of engineered nanomaterials in consumer products will increase the potential for their release to the environment. Carbon nanotubes (CNTs) have garnered significant attention due to their expected widespread usage (e.g., production of plastics, catalysts, water purification systems, and components in the electronics, aerospace and automotive industries [1]). CNTs are rolled up sheets of graphene composed of one or more concentric tubes (i.e., single-walled nanotubes (SWCNT) and multi-walled nanotubes (MWCNTs), respectively). Many MWCNTs are modified to make them stable in solution such as for biomedical applications,[7,8] which may make them more mobile in the environment. Moreover, some forms of modified carbon nanotubes are already commercially available. Inevitably some CNTs will eventually enter the environment through their disposal or from incidental release, yet their environmental transport behaviors are not yet well understood. In particular, they may enter soil ecosystems at high concentrations through land application of sewage sludge or from disposal of CNT-containing waste in landfills.[2] Although modern landfills have barrier systems, their effectiveness at containing CNTs is presently unknown and hence the potential for their migration through porous media in the subsurface is of considerable interest both with regards to potential ecotoxicological risks to soil organisms[3−6] and human health risks (e.g., contamination of drinking water supplies).

Traditional colloid filtration theory (CFT) is used to predict retention of particles in porous media systems due to gravitational sedimentation, Brownian diffusion, and interception.[9] This theory suggests that particles are transported to and become permanently deposited in the primary minimum well of a collector of uniform surface characteristics with infinite retention capacity.[9,10] Research suggests that additional removal mechanisms may be operative including deposition in the secondary minimum and surface charge heterogeneity.[10−14] It has been suggested that physical removal mechanisms (e.g., straining which is a function of particle to pore throat size) also play a role in the removal of colloidal particles from suspension,[15,16] and may be significant for nonspherical particles with large aspect ratios like CNTs.[17,18] Research on colloidal particles has also shown that the size of collectors may not only affect the degree of

Received: May 18, 2011
Accepted: September 28, 2011
Revised: September 25, 2011
Published: September 28, 2011

straining that may be operative but also affect the attachment of particles.[11,19] Evidence of site blocking, where the collector surface has a finite retention capacity, has also been observed in engineered nanoparticle studies.[20,21] Transport studies involving CNTs thus far have shown that CFT cannot fully describe their deposition behavior and one or more additional mechanisms are needed to explain experimental findings.[17,18,20,22−23]

While a large number of studies have investigated transport of SWCNTs,[17,18,20,22−23] relatively little work has been conducted to investigate MWCNT mobility. All SWCNT studies have used porous media with a mean collector diameter greater than 263 μm, although one study had a significant fraction of clay particles (29%).[17] The two experimental studies investigating the mobility of MWCNTs suggest that the deposition of MWCNTs in porous media can be described using an extension of CFT.[20,24] Enhanced mobility of acid-functionalized MWCNTs through porous media (quartz sand, d_{50} = 476 μm) was observed above a critical pore water velocity, but mobility was substantially decreased at pore water velocities similar to those expected in natural subsurface conditions.[20] Wang et al.[24] found that humic acid-stabilized MWCNTs (d = 35 nm) were filtered by quartz sand (d_{50} = 355 μm) to a greater extent than (humic acid-stabilized) SWCNTs (d = 1.4 nm) for all ranges of ionic strengths tested. The aforementioned studies investigating the mobility of CNTs show that their behavior is sensitive to many experimental conditions, but one important condition not yet investigated is the impact of porous media size on CNT transport. For example, no studies have investigated CNT mobility in porous media as fine as silt yet a wide range of porous media types and sizes are present in the subsurface.

The goal of this study was to investigate the impact of mean collector size, pore water velocity, and ionic strength on the mobility of MWCNTs. A series of one-dimensional column experiments were carried out at pore water velocities expected under both engineered and natural subsurface conditions using porous media ranging in classification from fine sand to silt. Manipulation of ionic strength facilitated an assessment of the relative importance of nontraditional filtration mechanisms (e.g., straining). Multiple pulses of MWCNTs were injected into the column to establish whether site blocking was operative and evaluate its importance to MWCNT transport.

MATERIALS AND METHODS

Multi-Walled Carbon Nanotubes. Multi-walled carbon nanotubes (MWCNTs) were purchased from Cheap Tubes Inc. (Brattleboro, VT). MWCNTs were functionalized through the addition of surface carboxylic and hydroxyl groups using a 3:1 v/v ratio of sulfuric (95−97%) and nitric acids (70%), respectively.[25] This treatment enhanced their hydrophilicity and stability in the aqueous phase. The solution was placed in a bath sonicator (Aquasonic Ultrasonic Cleaner, VWR Scientific Products, West Chester, PA) for 2 h. The functionalized MWCNTs were then collected using a 0.45 μm polytetraflouroethylene (PTFE) membrane. Boiling deionized water was used to rinse the MWCNTs until the filtrate had a neutral pH.[20] Finally MWCNTs were dried in a vacuum desiccator and stored until needed.

For column experiments, a dispersion of functionalized nanotubes was prepared by placing 4 mg of MWCNTs in a 250 mL beaker containing 200 mL of aqueous solution. An ultrasonic probe (Fisher Sonic Dismembrator, ARTEK System Corporation, Farmingdale, NY) was placed in the beaker, which was placed in an icewater bath, at 210 W for 45 min. The dispersed nanotubes were then mixed with an additional 300 mL of aqueous solution to reach the desired concentration of 8 mg/L. The MWCNT dispersions were left to sit for at least 24 h to allow the solution to equilibrate. Experiments were conducted immediately following this period, and nanotube agglomerates were not observed on the sides or bottoms of the beakers. Thus, 8 mg/L should be near the exact concentration given the lack of settling, but other minor forms of nanotube loss such as aerosolization during the sonication process cannot be excluded. These MWCNTs were thoroughly characterized using thermal gravimetric analysis, X-ray photoelectron spectroscopy, and scanning electron microscopy (see Supporting Information (SI) for additional details on the characterization methods).

Porous Media. Four quartz sands of varying grain size (Barco, Opta Minerals Inc. Waterdown, ON) were used (SI Table S1). The f32 and f71 sands (Barco #32 and Barco #71) size distributions were as received from the manufacturer. However, the 290 fractions 1 and 2 sands were obtained by sieving Barco #290 sand; 290 fraction 1 was the combination (1:4) of the fractions retained on the Tyler (Mentor, OH) no. 140 and Tyler no. 200 sieves while 290 fraction 2 was from sand retained on the Tyler no. 325 sieve. The sands are herein referred to by their d_{50} value to avoid confusion between the 290 fractions. The quartz sand was cleaned by washing with hydrochloric acid (0.1M) followed by hydrogen peroxide (5%) to remove any impurities from the surface of the sand grains. The sand was rinsed repeatedly with deionized water following both the acid and peroxide washing steps to ensure that all impurities had been removed from the sand and neutral pH had been achieved. The sand was then oven-dried (90 °C) overnight, following rinsing, and stored. Zeta potential of the porous media, quantified by streaming potential measurement (Anton Paar SurPASS system, Saint Laurent, Canada) using aqueous solution AS1b, were negative (i.e., ~ -50 mV). This suggests repulsive interactions between the CNTs and porous media.

Aqueous Solution Chemistry. Three aqueous solutions were employed all with a pH of approximately 7.5. The first high ionic strength solution (AS1) had an ionic strength of 7.5 mmol/L and was buffered to pH 7.5 with 1.26 mmol/L monosodium phosphate ($NaH_2PO_4.H_2O$), 1.73 mmol/L (Na_2HPO_4) and 1 mmol/L NaBr. The background aqueous solution (i.e., no MWCNTs) used in the high ionic strength column experiments (AS1b) had the same amount of phosphate as AS1 with the addition of 1 mmol/L NaCl instead of NaBr to act as a conservative tracer. The low ionic strength solution (AS2) (0.1 mmol/L) was obtained through dilution of AS1. In the column experiments at low ionic strength, the background solution was the same as the MWCNT solution, but without MWCNTs.

Column Experiments. Glass columns (2.5 cm in diameter and 5 cm in length) were used in this study. A stainless steel mesh (66 μm openings) followed by a nylon screen (25 μm openings), at column ends, were used to support the porous media and evenly distribute aqueous flow through the column (see Supporting Information for additional details on column packing). Columns were flushed with the appropriate background solution for 10 pore volumes following 30 pore volumes flushing with DI water. Flow in the 100% water saturated columns was then reduced to the experimental flow rate for at least one pore volume and the direction of flow was switched to vertically downward. Following the flow reversal, MWCNT solutions were injected into the column. Multiple 60 mL plastic syringes and a

syringe pump (KD Scientific, Holliston, MA) were used for solution injection. Two pulses of MWCNTs were injected with sufficient time between pulses to allow column effluent absorbance to reach background levels.

Once the absorbance of the column effluent had reached background levels after the second MWCNTs pulse, deionised water was flushed through the column to determine if the sudden drop in ionic strength would mobilize MWCNTs that may have been deposited on the sand grains. The column effluent was collected using a CF-1 fraction collector (Spectrum Chromatography, Houston, TX) and the MWCNT concentration determined using a UV spectrophotometer (Helios Alpha, Thermo Fisher Scientific, Mississauga, ON) at a wavelength of 400 nm. A calibration curve of MWCNT concentration versus absorbance was highly linear at this wavelength with $R^2 > 0.997$. Conservative tracer concentrations (NaBr) were quantified using high performance liquid chromatography (HPLC, Waters Company, Milford, MA) of the collected fractions.

Mathematical Modeling of MWCNT Transport. A one-dimensional finite element model was used to simulate MWCNT transport.[20] The simulator was based on traditional colloid filtration theory but was modified to include site blocking and dual deposition. Please see the SI for additional numerical modeling details.

RESULTS AND DISCUSSIONS

MWCNT Characterization. Thermal gravimetric analysis results indicated that the catalyst impurities were only (0.8 ± 0.1) % (n = 4) of the MWCNTs; thus, metal impurities were almost completely removed (SI Figure S1). The lack of a peak at a lower temperature than the principal peak indicated a lack of amorphous carbon. X-ray photoelectron spectroscopy (XPS) (see SI Figure S2) indicated that (6.2 ± 1.4) % of the MWCNTs was oxygen, a result similar to that obtained with MWCNTs treated with the same acid modification process in a prior study.[26] These oxygen functional groups and a related scan of the C (1s) region indicated the presence of carboxyl and hydroxyl functional groups. A previous study indicated that ultrasonication of an MWCNT solution without an ice−water bath for 6 h only caused a slight increase in the oxygen content from 7.5% to 8.6%.[27] Thus, the 45 min sonication in an ice−water bath used here is not expected to substantially increase the concentration of functional groups on the MWCNTs. According to scanning electron microscopy, the measured MWCNT outer diameter was 36 ± 11 nm (n = 132), and length was 540 ± 340 nm (n = 215) (see SI Figures S3 and S4). While the diameters matched the manufacturer's specifications, the lengths were substantially shorter than the 10−20 μm indication by the manufacturer. It was unclear if this discrepancy was a result of the sonication process or acid functionalization or if the MWCNTs were originally shorter than indicated by the manufacturer. Regardless, this result further affirms the importance of in-depth nanoparticle characterization prior to environmental behavior experiments.[28−30]

Column Experiments. Column experiments were conducted to assess the impact of collector grain size on the transport and deposition of MWCNTs. Column experiments were first conducted at a higher pore water velocity (4.9×10^{-5} m/s or 4.2 m/d) using AS1 to disperse the MWCNTs and AS1b as the background solution. The first MWCNT pulse exited the column noticeably later than the conservative tracer (NaBr) with the extent of retardation increasing with decreasing collector size (Figure 1). Following breakthrough the MWCNT normalized effluent concentration increases relatively quickly but slows at a normalized effluent concentration of approximately 0.65. After approaching or reaching a plateau injection of MWCNTs ceased and background solution injection commenced. After MWCNT injections stopped, the normalized MWCNT effluent concentrations decreased with the conservative tracer for both pulses and for both pore water velocities (Figures 1 and 2).

MWCNT breakthrough was significantly different for the second pulse. The maximum normalized concentrations for the (476, 175, and 80) μm sands were about 0.8 for both pulses, while the effluent concentration for the 50 μm sand packed column reached an effluent concentration of 0.65 with the conservative tracer and then gradually rose to a maximum value of 0.75 more slowly than the tracer (Figure 1).

The results observed here differ from those for humic acid-stabilized MWCNTs for which MWCNT breakthrough occurred ahead of the conservative tracer at all ionic strengths investigated.[24] The pore velocity used in their study was similar (8.9×10^{-5} m/s or 7.7 m/d) to the higher velocity used in the current study and the mean grain size was in the same range (d_{50} = 350 μm). Given that their diameters ((35 ± 10) nm, length not reported) were similar to the MWCNT tested here, these observed differences are likely due to different stabilization methods and the resultant differences in interaction energies.

At the lower pore velocity (4.9×10^{-6} m/s or 0.42 m/d), MWCNT transport was similar to that observed in the high velocity experiments in the following ways: (i) the conservative tracer exits the column more quickly than the MWCNTs; (ii) the MWCNTs show increased retardation with decreasing collector grain size; (iii) MWCNT normalized effluent concentration increased at a relatively fast rate initially until a steady state effluent concentration was achieved for some experimental conditions, while in other cases effluent concentrations increased at a much slower rate until injection of MWCNT ceased; and (iv) limited MWCNT retardation was observed for the second pulse but this was more observable than during the high velocity experiments (Figures 1 and 2). The maximum normalized concentration obtained for the (476, 175, and 80) μm sands after a second MWCNT pulse were again similar (0.65). For the second pulse, MWCNTs exhibited a slightly delayed breakthrough in the 50 μm sand compared to the conservative tracer and reached a maximum value of 0.5 (Figure 2d). It is important to note that the MWCNTs are still mobile in the finest porous media fraction, which would be classified as silt.

Upon completion of the second pulse, deionized water was injected into the columns at the experimental flow rate. For all experiments this resulted in a sharp and reproducible spike in effluent absorbance (e.g., Figure 3) suggesting that a fraction of the MWCNTs that were loosely deposited on collector surfaces had been remobilized.[18] This release has been attributed to the increase in electrostatic repulsion due to the elimination of the secondary energy minimum by lowering the ionic strength from 7.5 mM to that of deionized water.[18] The amount of MWCNTs released from the porous media did not follow any specific trend with respect to collector diameter. Jaisi et al.[18] reported that the concentration released from collector surfaces in this manner generally increased following experiments of increasing ionic strength (i.e., high experiment ionic strength leads to higher concentration of CNT in the effluent following the deionized solution flush).[18] In the current study, the same trend was observed, because MWCNTs were not released upon injection

of deionized water in low ionic strength (0.1 mM) experiments (Figure 4). This result is likely attributable to the relatively small change in ionic strength between the 0.1 mM solution and deionized water and the negligible secondary minimum at the low ionic strength.

A suite of experiments were conducted at the low pore velocity (4.9×10^{-6} m/s or 0.42 m/d) and low ionic strength (0.1 mM) to see if nonphysiochemical removal mechanisms (e.g., straining) were operative (Figure 4). In all cases MWCNTs exited the column at the same time and at a similar rate as the representative tracer in the high ionic strength experiments (Figure 4) (i.e., no retardation of either pulse). When the background solution flush was initiated, MWCNT effluent concentrations exited the column in a similar manner to representative tracer concentrations. The maximum normalized effluent concentration was approximately 0.95 except in the case of the 50 μm sand, which had a maximum normalized effluent concentration of approximately 0.9. Given the relatively large repulsive barrier that exists at the low ionic strength, any MWCNT removal was likely due mechanisms other than those associated with traditional filtration theory. One possible nonphysiochemical removal mechanism that may be of importance is straining,[31] although given that normalized effluent concentrations are above 0.9 for the low ionic strength solution, this would suggest it is not a dominant retention mechanism. Liu et. al.[20] observed a maximum normalized effluent concentration of MWCNTs of approximately 0.65

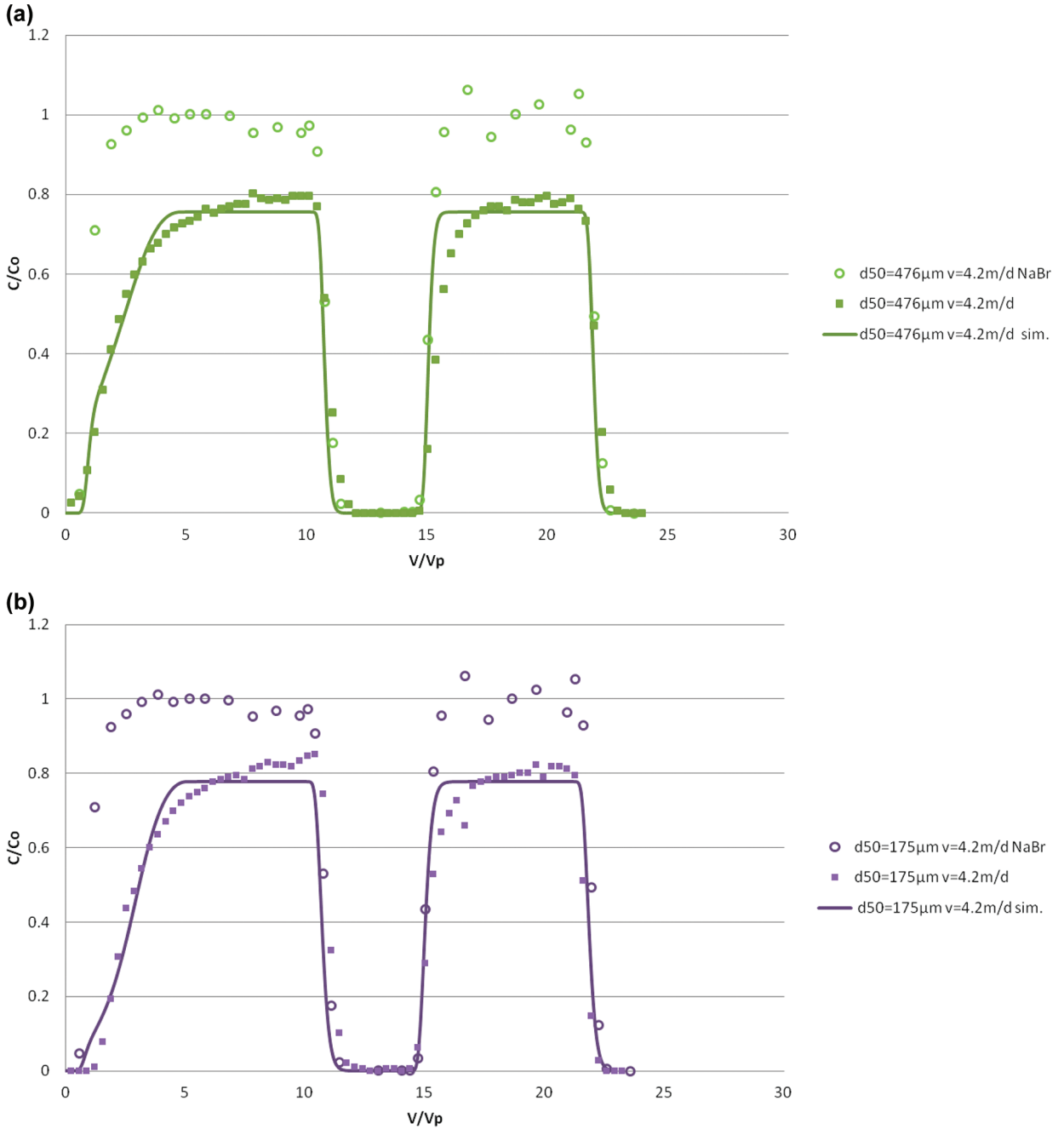

Figure 1. Continued

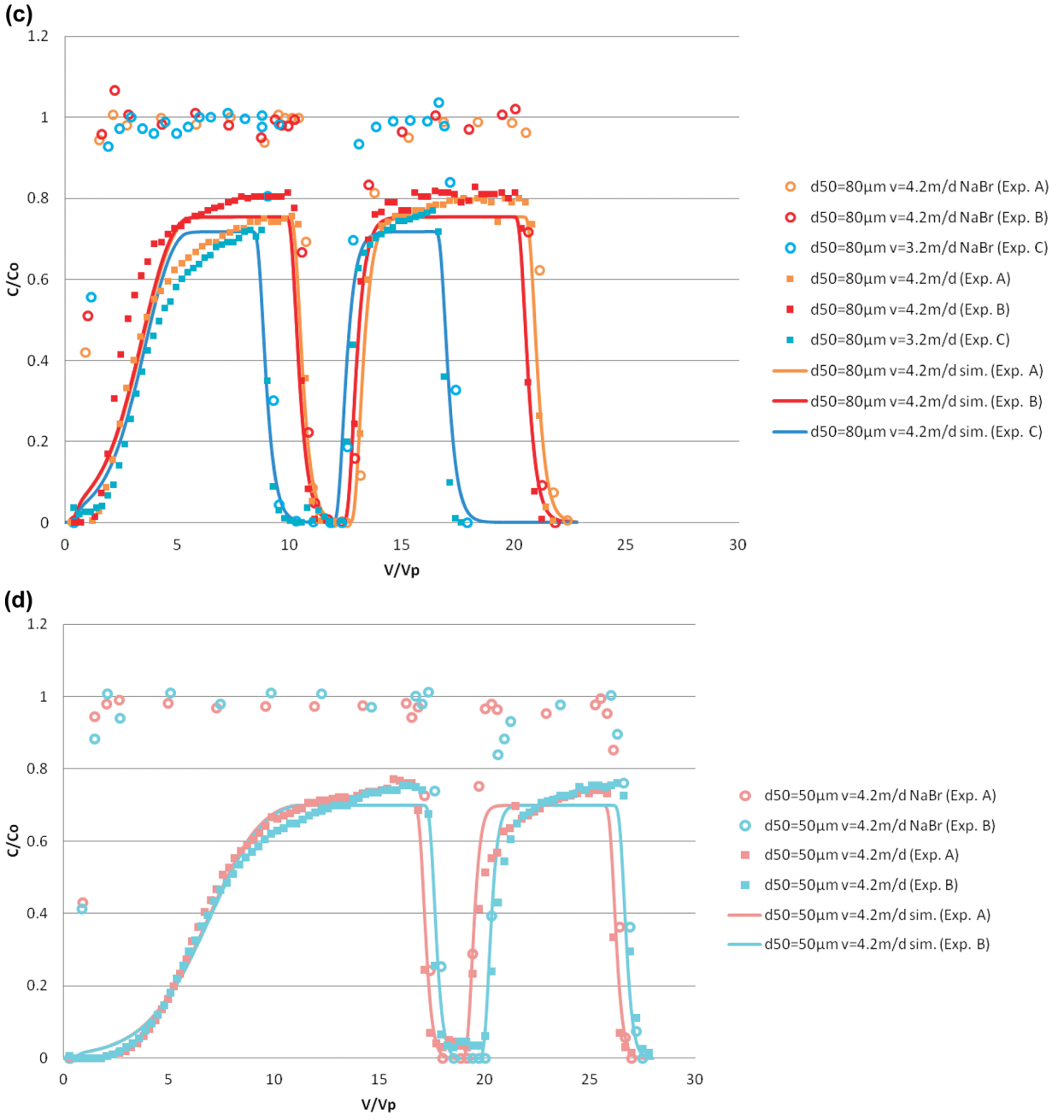

Figure 1. Breakthrough curves of MWCNTs at the high pore water velocity, $I = 7.5$ mmol/L in (a) 476 μm, (b)175 μm, (c) 80 μm and (d) 50 μm sand packed columns. Open circles represent conservative tracer data, squares represent MWCNT data and solid lines represent the results of simulation (noted as sim.). Experiments A, B, and C are replicates. RMSE values provided in SI Table S2 provide estimates of the quality of the modeling fits.

at an ionic strength of 0.1 mM which was similar to the maximum concentration achieved at the high ionic strength (10 mM) in that study. This difference from our results may be due to significant nonphysiochemical removal occurring at the low ionic strength.[20]

The results obtained at the low ionic strength case (0.1 mmol/L) in this study were similar in shape and appearance to those obtained in a previous study using SWCNTs.[18] In that study, SWCNTs exited the column with the conservative tracer and reached a maximum normalized effluent concentration of approximately 0.93. In a different study, higher than expected removal occurred at low ionic strengths which was attributed to straining rather than filtration of the CNTs.[17] Along these lines, Jaisi et al.[18] observed a decrease in the hydrodynamic diameter in the SWCNT fraction that passed through the column, and postulated that this decrease may be due to larger particles being removed in the column due to straining; while dynamic light scattering (DLS) has limitations for CNTs as a result of the assumption that the particles are monodisperse spheres in the fitting algorithm, it was helpful for comparing relative differences among these fractions. In this study, the influent MWCNT suspension had an average effective diameter of 188 nm, measured by DLS, and an average effective effluent diameter of 176 nm. Given the relatively small change in effective diameter, straining appears to be a relatively minor mechanism.

Another method to assess if straining is a dominant removal mechanism is to quantify the ratio of a representative particle diameter and a representative pore throat diameter (L/L), usually taken to be d_{50}.[32] The critical ratio was previously proposed to be 0.003.[31] A study using SWCNTs reported ratios of 0.0008 and 4.7×10^{-6} for the SWCNT effective diameter and SWCNT diameter, respectively,[18] whereas an MWCNT transport study had a ratio of 0.0001.[20] The straining ratio using the length (0.0011 to 0.011) and the MWCNT diameter (0.00008−0.0007) in this study are below the critical ratio proposed of 0.003 for diameter but not length.

Traditionally, the porous media is treated as a "clean bed" which means that particle deposition rate is constant.[33] Site blocking, which occurs when the deposition rate decreases over time (i.e., less particles are deposited onto the collector surface as it becomes covered by particles),[34] has been observed in other nanoparticle transport studies.[20,21] Given the retarded MWCNT breakthrough for the first pulse, and not the second pulse, in all high ionic strength experiments, this suggests that site blocking may be an operative mechanism (Figures 1 and 2). The shape of the breakthrough curves also provides evidence for the occurrence of site blocking as the deposition rate does change with continued MWCNT transport through the column (i.e., there is no stable steady state effluent concentration in some experiments but rather the maximum normalized concentration slowly increases as the deposition rate drops). These observations are consistent with previous research that has suggested site blocking was operative.[21,32,34−36]

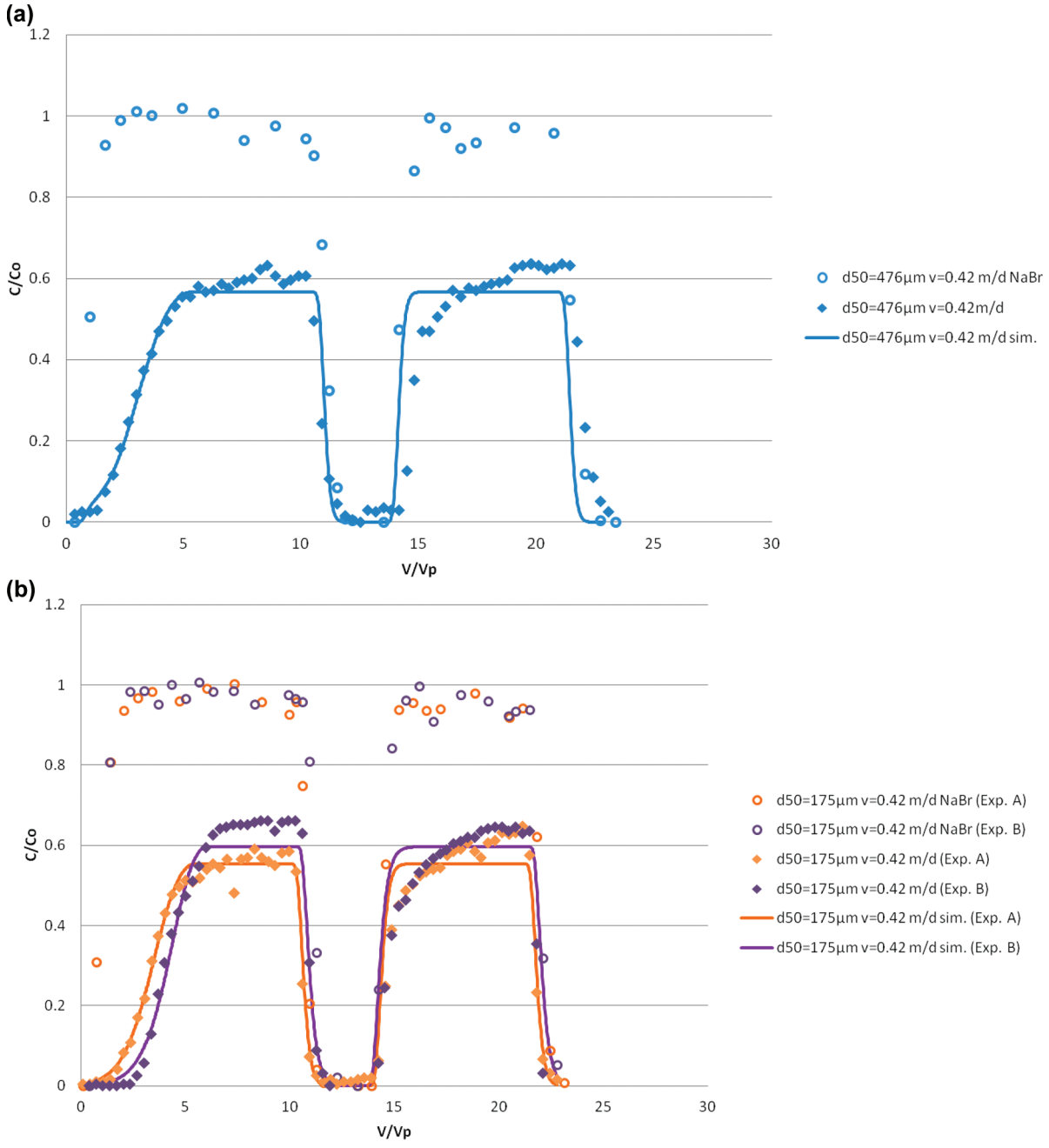

Figure 2. Continued

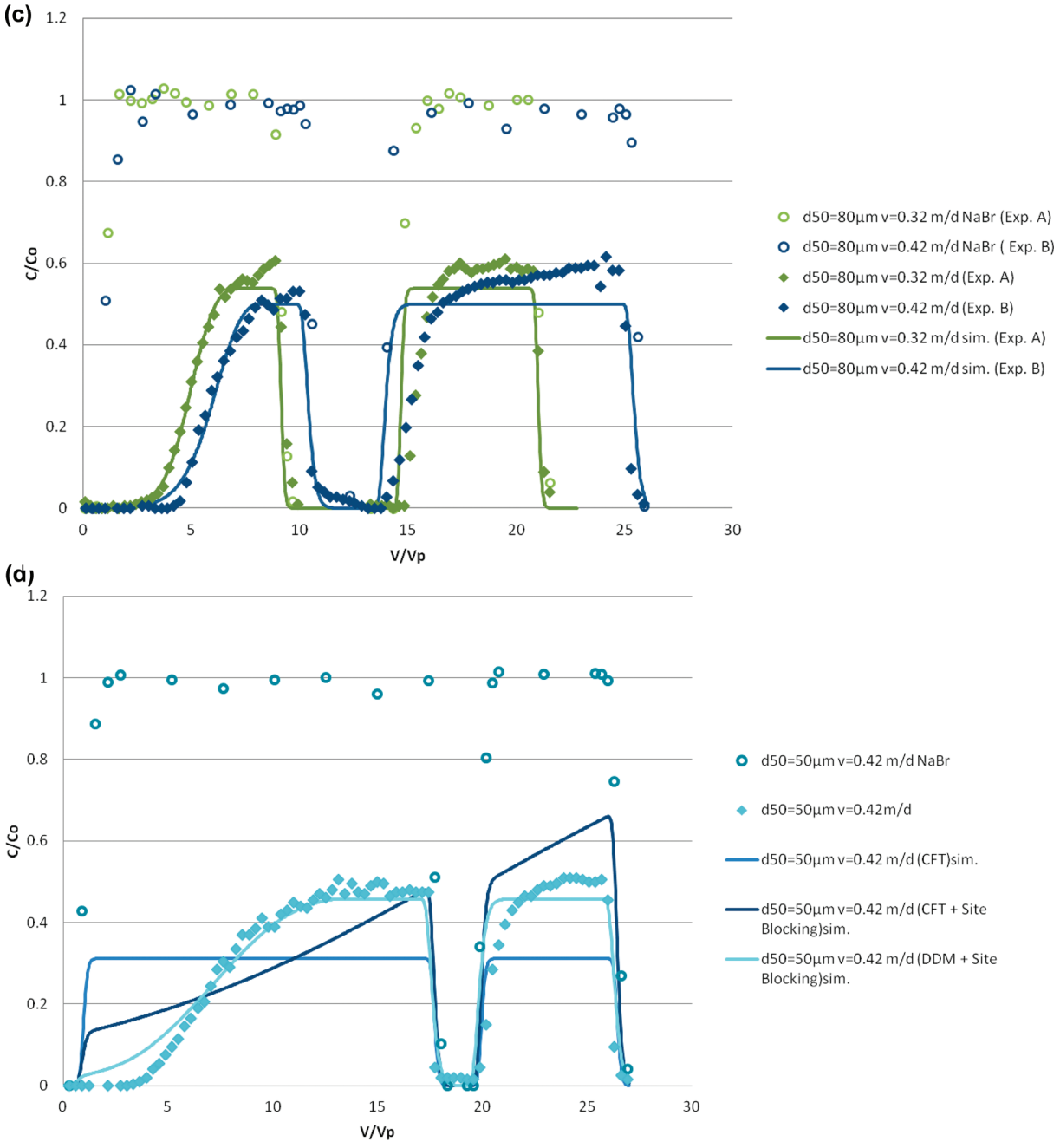

Figure 2. Breakthrough curves of MWCNTs at the low pore water velocity I = 7.5 mmol/L in (a) 476 μm, (b)175 μm, (c)80 μm, (d) 50 μm sand packed columns. Open circles represent conservative tracer data, diamonds represent MWCNT data and solid lines represent the results of simulation (noted as sim.) For Figure 2d simulated lines represent mechanisms associated with traditional colloid filtration theory (CFT); traditional colloid filtration theory with site blocking (CFT + site blocking) and dual deposition with site blocking (DDM + site blocking) Experiments A and B are replicates. RMSE values provided in SI Table S2 provide estimates of the quality of the modeling fits.

RESULTS OF NUMERICAL SIMULATION

A series of simulations were conducted to test the ability of the numerical simulator to reproduce observed high ionic strength experiments (I = 7.5 mmol/L), using traditional CFT and modified versions of CFT. It was assumed that there was no detachment of MWCNTs from the sand surface (i.e., k_{det} = 0) as no tailing was observed in any of the experiments. Initially simulations only incorporated mechanisms traditionally associated with CFT (i.e., assuming ψ = 1 and α_{ii} =0, eqs 2 and 4 in SI) and α_i and α_1 were fitted. Model results suggest that MWCNTs break through with the conservative tracer and achieve an effluent concentration plateau of 0.3 (Figure 2d, other results not shown due to space limitations). Observed behaviors, which exhibited significant MWCNT retardation for the first pulse, were significantly different than these simulation results. This suggests that clean bed behavior, where an effluent steady state concentration is rapidly achieved and maintained for the duration of particle injection, could not adequately describe observed experimental

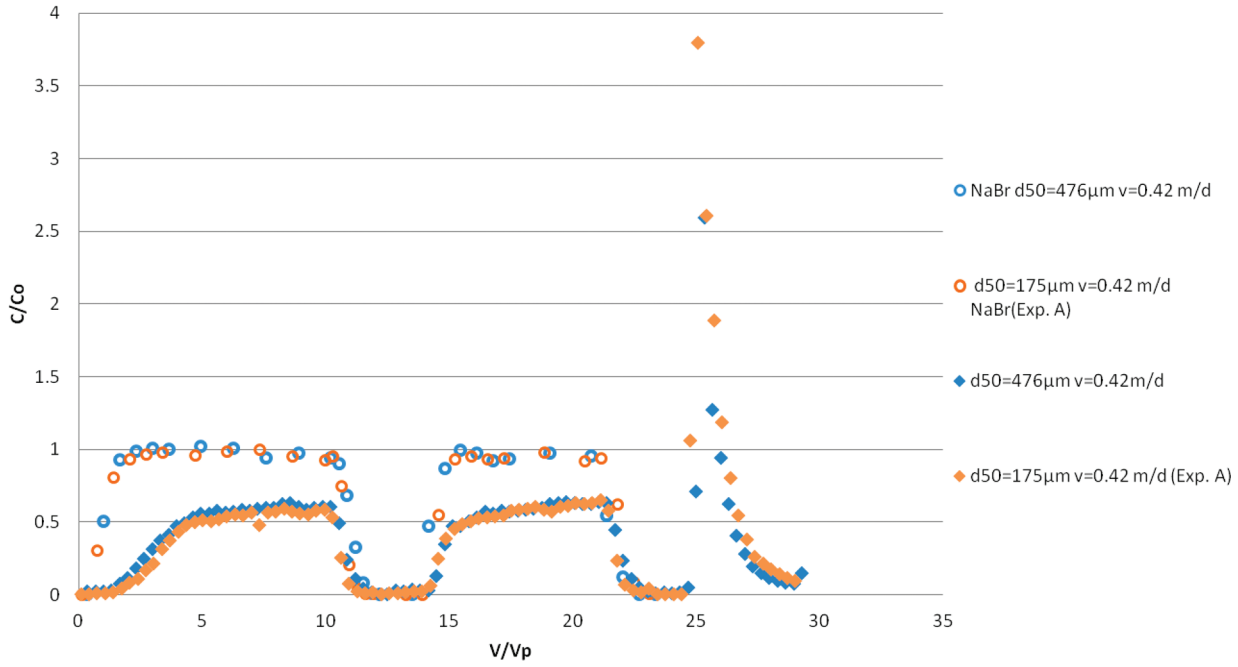

Figure 3. Breakthough curves of MWCNTs including elution with deionized water (third pulse on graph). Open circles represent conservative tracer data, diamonds represent MWCNT data.

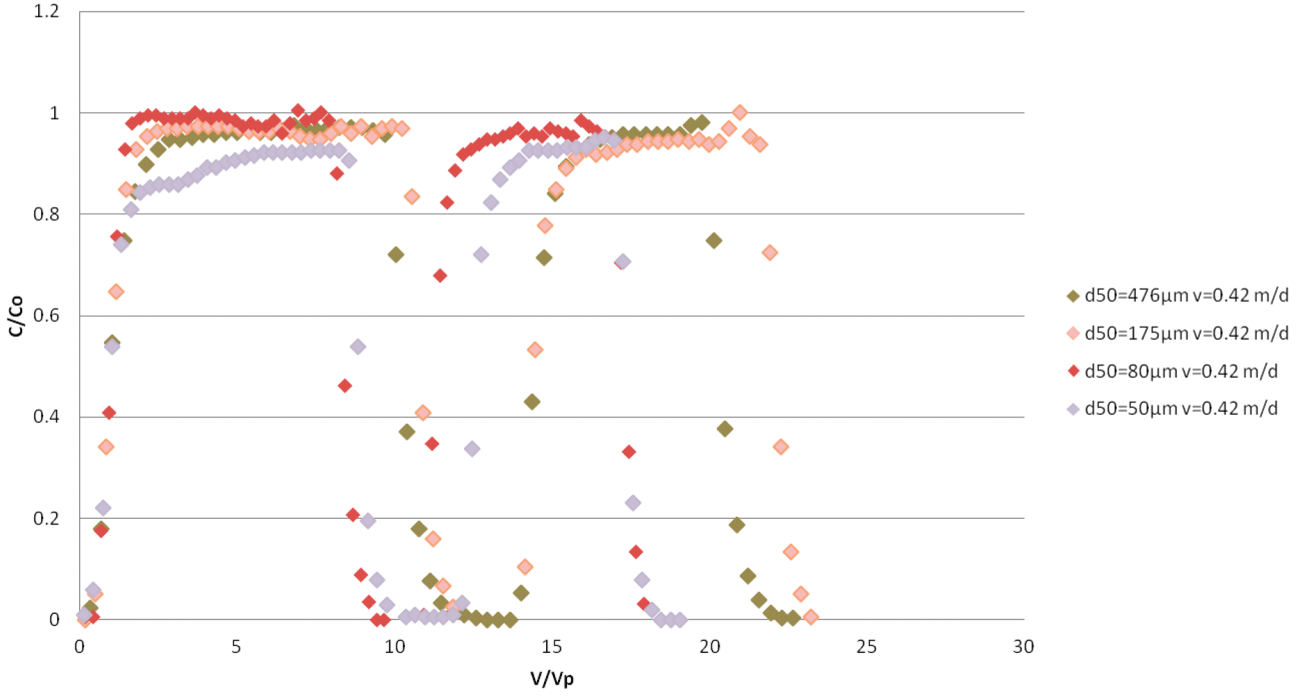

Figure 4. Breakthrough curves of MWCNTS for low ionic strength (0.1 mmol/L) experiment through (476, 175, 80, and 50) μm sand packed columns.

results. For comparison with subsequent simulations, the root-mean-square error (RMSE) value of this analysis was 0.167 (SI Table S2).

As previously discussed, observed MWCNT transport behaviors (Figures 1a−d and 2a−d) suggest site blocking may be operative. A site blocking function (ψ in eq 2) was therefore incorporated in the governing mass balance equations to account for this observed behavior. This form of ψ suggests that as S approaches S_{max} the blocking function approaches zero. This means that once the surface becomes covered by deposited MWCNTs, attachment will cease and the normalized MWCNT effluent concentration will increase to one. The blocking function would be particularly useful in describing the reduction in MWCNT retardation between the first and second pulses, and

dx.doi.org/10.1021/es2017076 |*Environ. Sci. Technol.* 2011, 45, 9765–9775

the non clean bed plateau observed in some cases where the normalized concentration of MWCNTs slowly increases with time (Figures 1 and 2).

For these simulations the values of α_i, S_{max}, and α_1 were fitting parameters (i.e., assuming $\alpha_{ii} = 0$). The inclusion of site blocking significantly improved the fit to experimental results (RMSE = 0.117), but the model still did not predict MWCNT retardation (Figure 2d). Furthermore, MWCNT concentrations are overestimated until 6.7 pore volumes at which point the model underpredict the normalized effluent concentration of MWCNTs in the first pulse. The model also overpredicted the MWCNT concentration during the second pulse.

Based on the site blocking function adopted, as more MWCNTs were injected into the column, the magnitude of the blocking term should decrease and thus the plateau of the second pulse should have been higher than the first pulse due to lower deposition rate as fewer sites remained available for deposition. However, this was not the case, and thus these model results suggest that the site blocking function cannot account for the similar height of the first and second pulses and that, along with retention at a finite number of sites, other deposition mechanisms may be operative. Straining is one such mechanism, but based on the results of the low ionic strength experiments, was likely not a dominant process. Dual deposition, a process which may be due to deposition of particles in the secondary energy minimum and surface charge heterogeneity,[13] was thus considered. Results from the deionized water flush, following the second MWCNT pulse, support the presence of a secondary energy minimum (Figure 3). Previous studies have used this type of model to simulate similar experimental behavior.[13,37] Tufenkji et al.[13] found that both favorable and unfavorable sites may be present on collector surfaces. As such favorable and unfavorable deposition of particles can occur simultaneously, where a fraction of the particles experience a fast deposition rate while others experience a slow deposition rate.

To account for a dual deposition model (DDM), a second removal rate constant ($k_{att,ii}$) was incorporated into the solid phase mass balance equation (eq 2). The site blocking function ψ was only applied to the fast deposition rate and it was assumed that site blocking did not play a significant role in slow deposition. Inclusion of DDM and the site blocking term significantly improved agreement between the numerical model and experimental results (RMSE = 0.053, Figure 2d). Model results are in similar good agreement with experimental observations for all of the experimental data (i.e., both velocities) when both DDM and a site blocking term are incorporated in the governing mass balance equations (Figures 1 and 2). Fitted parameters are presented in Table S2 in the SI.

The values of S_{max} obtained in this study were similar in magnitude to previous results for fullerene particles,[21] but were an order of magnitude greater than results obtained previously for MWCNTs.[20] This suggests that the collector surfaces have significantly larger capacities for the MWCNTs used in this study in comparison to the MWCNTs used previously.[20] At both high and low pore water velocities, S_{max} increases as the average collector grain size decreases consistent with results reported in the fullerene nanoparticle transport study.[21] The increase in S_{max} with decreasing grain size is likely due to the increased surface area of collectors and corresponding total number of depositional sites. S_{max} is an exponential function of specific surface area of collectors (surface area of sphere with diameter equal to the d_{50} of the soil divided by its volume) (SI Figure S5). Li et al.[21] reported an increase in S_{max} as pore velocity decreases, for the same collector sizes, consistent with the results reported here. The reduction in S_{max} associated with increased pore water velocity may be due to increased tangential velocities across the collector surface which creates a "shadow effect" down gradient of the collector due to hydrodynamic scattering.[34,38] It should be noted that S_{max} is a weaker function of pore water velocity than collector size.

$k_{att,i}$ and $k_{att,ii}$ increase with increasing pore water velocity consistent with previous CNTs transport studies [17,20] (SI Table S2). $k_{att,i}$ and $k_{att,ii}$ also generally increased with decreasing mean collector size. The impact of collector size on $k_{att,i}$ and $k_{att,ii}$ was less than that of pore water velocity. Attachment efficiency (α), the total number of attachments to the total number of collisions between the MWCNT particles and collectors, was calculated from fitted attachment rates ($k_{att,i}$ and $k_{att,ii}$) and estimated single collector efficiencies formulated based on mechanisms associated with traditional CFT[20] (SI Table S2). Attachment efficiency decreased with pore water velocity and with mean grain size. Values ranged between 0.01 and 1.20, with the value greater than unity for the 476 μm sand at 4.2 m/d. The value greater than unity may be attributed to shortcomings of the single collector efficiency (η_0) relationship used in this study or that unique, mean values for key MWCNT and soil properties were used in the calculation. Historically, attachment efficiency was assumed to only be related to chemical factors (e.g., ionic strength, pH),[9] but recent studies suggest that the attachment is also a function of hydrodynamic factors.[10,39−41] Shen et al.[10] showed that when hydrodynamic factors are not considered (i.e., only Derjaguin−Landau−Verwey−Overbeek (DLVO) interactions and Brownian diffusion were considered), the attachment efficiency was overestimated. Additional mechanisms (hydrodynamic effects and van der Waals interactions)[42] should likely be included in η_0 and may reduce α below unity. Although inclusion of a DDM and a site blocking term considerably improved model agreement with experimental results, the agreement is not perfect. A number of simplifying assumptions were made in conceptual model development (i.e., unique porous media grain size and carbon nanotube dimensions). Solution of a more complex conceptual model would likely improve agreement between model and experimental results.

These fitted parameters suggest that under the conditions investigated the maximum travel distance of MWCNTs (calculated as the distance needed to reduce the effluent concentration of MWCNTs to 0.1% of the initial concentration) observed decreases from 1.2 m in fine sand to 0.9 m in silts (SI Table S2) at the higher pore water velocity. These distances are obtained from values of $k_{att.ii}$, but it is unknown if deposition sites associated with this term are subject to site blocking which could significantly increase travel distances of MWCNTs.

■ ENVIRONMENTAL IMPLICATIONS

Results from this study suggest that commercially available MWCNTs are mobile in porous media with collector sizes ranging from fine sands to silt. Differences in breakthrough curves between the first and second pulses indicate that the deposition rate decreases as the experiment progresses and that site-blocking may be operative. These results could not be predicted using traditional CFT. However, a dual deposition model with a site blocking term significantly improved agreement between experimental observations and model results.

Increased MWCNT retardation with decreasing collector size was likely due to the increased surface area and depositional sites. Nonphysiochemical removal mechanisms (e.g., straining) may influence MWCNTs deposition, but low ionic strength (0.1 mmol/L) results suggest that this contribution is minor.

These findings are based on fundamental experiments incorporating ideal porous media systems. The inclusion of organic matter, divalent cations (e.g., Ca^{2+} or Mg^{2+}) and both chemical and physical heterogeneity, as would be expected in subsurface environments, would impact the mobility of MWCNTs and are important topics for additional research. Moreover, the CNTs used in this manuscript were functionalized to make them more stable in solution. Nonfunctionalized may exhibit different transport behaviors. More research is needed to fully understand the complexities of CNT transport. Findings suggest that site blocking may increase the overall travel distances of MWCNTs in the subsurface beyond what is expected from traditional CFT. This study does highlight the importance of collector size on MWCNT transport and shows that MWCNTs are mobile through increasingly finer material which are present in subsurface environments. Further work is necessary to assess the toxicity of CNTs that could be dispersed in aqueous solutions, be mobile in subsurface systems, as suggested in this study, and contaminate aquifers used as sources of drinking water.

■ ASSOCIATED CONTENT

Supporting Information. Additional experimental methods, MWCNT characterization data, comparison of S_{max} and specific surface area of sands, summary figures for the first pulse at the higher and lower velocities, summary of model parameters, and a summary of experiments. This material is available free of charge via the Internet at http://pubs.acs.org.

■ AUTHOR INFORMATION

Corresponding Author
*Phone: (519)-661-2198; e-mail: docarroll@eng.uwo.ca.

■ ACKNOWLEDGMENT

Certain commercial equipment or materials are identified in this paper in order to specify adequately the experimental procedure. Such identification does not imply recommendation or endorsement by the National Institute of Standards and Technology, nor does it imply that the materials or equipment identified are necessarily the best available for the purpose. This research was supported by an Ontario Ministry of the Environment Best in Science Award, the Natural Sciences and Engineering Research Council of Canada and the Canadian Foundation for Innovation. We thank Howard Fairbrother for his helpful advice on MWCNT stability.

■ REFERENCES

(1) Klaine, S. J.; Alvarez, P. J. J.; Batley, G. E.; Fernandes, T. F.; Handy, R. D.; Lyon, D. Y.; Mahendra, S.; McLaughlin, M. J.; Lead, J. R. Nanomaterials in the environment: Behavior, fate, bioavailability, and effects. *Environ. Toxicol. Chem.* **2008**, *27* (9), 1825–1851.

(2) Gottschalk, F.; Sonderer, T.; Scholz, R. W.; Nowack, B. Modeled Environmental concentrations of engineered nanomaterials (TiO_2, ZnO, Ag, CNT, fullerenes) for different regions. *Environ. Sci. Technol.* **2009**, *43* (24), 9216–9222.

(3) Petersen, E. J.; Huang, Q. G.; Weber, W. J. Relevance of octanol-water distribution measurements to the potential ecological uptake of multi-walled carbon nanotubes. *Environ. Toxicol. Chem.* **2010**, *29* (5), 1106–1112.

(4) Petersen, E. J.; Huang, Q. G.; Weber, W. J. Bioaccumulation of radio-labeled carbon nanotubes by Eisenia foetida. *Environ. Sci. Technol.* **2008**, *42* (8), 3090–3095.

(5) Petersen, E. J.; Pinto, R. A.; Landrum, P. F.; Weber, W. J. Influence of carbon nanotubes on pyrene bioaccumulation from contaminated soils by earthworms. *Environ. Sci. Technol.* **2009**, *43* (11), 4181–4187.

(6) Petersen, E. J.; Pinto, R. A.; Zhang, L. W.; Huang, Q. G.; Landrum, P. F.; Weber, W. J. Effects of Polyethyleneimine-mediated functionalization of multi-walled carbon nanotubes on earthworm bioaccumulation and sorption by soils. *Environ. Sci. Technol.* **2011**, *45* (8), 3718–3724.

(7) Shen, M. W.; Wang, S. H.; Shi, X. Y.; Chen, X. S.; Huang, Q. G.; Petersen, E. J.; Pinto, R. A.; Baker, J. R.; Weber, W. J. Polyethyleneimine-mediated functionalization of multi-walled carbon nanotubes: Synthesis, characterization, and in vitro toxicity assay. *J. Phys. Chem. C* **2009**, *113* (8), 3150–3156.

(8) Shi, X. Y.; Wang, S. H.; Shen, M. W.; Antwerp, M. E.; Chen, X. S.; Li, C.; Petersen, E. J.; Huang, Q. G.; Weber, W. J.; Baker, J. R. Multifunctional dendrimer-modified multi-walled carbon nanotubes: Synthesis, characterization, and in vitro cancer cell targeting and imaging. *Biomacromolecules* **2009**, *10* (7), 1744–1750.

(9) Yao, K. M.; Habibian, M. M.; Omelia, C. R. Water and waste water filtration—Concepts and applications. *Environ. Sci. Technol.* **1971**, *5* (11), 1105–1112.

(10) Shen, C.; Li, B.; Huang, Y.; Jin, Y. Kinetics of Coupled Primary- and Secondary-Minimum Deposition of Colloids under Unfavorable Chemical Conditions. *Environ. Sci. Technol.* **2007**, *41* (20), 6976–6982.

(11) Shen, C. Y.; Huang, Y. F.; Li, B. G.; Jin, Y., Predicting attachment efficiency of colloid deposition under unfavorable attachment conditions. *Water Resour Res* **2010**, *46*, -.

(12) Elimelech, M.; Omelia, C. R. Effect of particle-size on collision efficiency in the deposition of brownian particles with electrostatic energy barriers. *Langmuir* **1990**, *6* (6), 1153–1163.

(13) Tufenkji, N.; Elimelech, M. Deviation from the classical colloid filtration theory in the presence of repulsive DLVO interactions. *Langmuir* **2004**, *20* (25), 10818–10828.

(14) Tufenkji, N.; Elimelech, M. Breakdown of colloid filtration theory: Role of the secondary energy minimum and surface charge heterogeneities. *Langmuir* **2005**, *21* (3), 841–852.

(15) Bradford, S. A.; Yates, S. R.; Bettahar, M.; Simunek, J., Physical factors affecting the transport and fate of colloids in saturated porous media. *Water Resour Res* **2002**, *38*, (12), 1327.

(16) Bradford, S. A.; Bettahar, M.; Simunek, J.; van Genuchten, M. T. Straining and attachment of colloids in physically heterogeneous porous media. *Vadose Zone J* **2004**, *3* (2), 384–394.

(17) Jaisi, D. P.; Elimelech, M. Single-walled carbon nanotubes exhibit limited transport in soil columns. *Environ. Sci. Technol.* **2009**, *43* (24), 9161–9166.

(18) Jaisi, D. P.; Saleh, N. B.; Blake, R. E.; Elimelech, M. Transport of single-walled carbon nanotubes in porous media: Filtration mechanisms and reversibility. *Environ. Sci. Technol.* **2008**, *42* (22), 8317–8323.

(19) Torkzaban, S.; Bradford, S. A.; Walker, S. L. Resolving the coupled effects of hydrodynamics and DLVO forces on colloid attachment in porous media. *Langmuir* **2007**, *23* (19), 9652–9660.

(20) Liu, X. Y.; O'Carroll, D. M.; Petersen, E. J.; Huang, Q. G.; Anderson, C. L. Mobility of multi-walled carbon nanotubes in porous media. *Environ. Sci. Technol.* **2009**, *43* (21), 8153–8158.

(21) Li, Y. S.; Wang, Y. G.; Pennell, K. D.; Abriola, L. M. Investigation of the transport and deposition of fullerene (C60) nanoparticles in quartz sands under varying flow conditions. *Environ. Sci. Technol.* **2008**, *42* (19), 7174–7180.

(22) Lecoanet, H. F.; Wiesner, M. R. Velocity effects on fullerene and oxide nanoparticle deposition in porous media. *Environ. Sci. Technol.* **2004**, *38* (16), 4377–4382.

(23) Lecoanet, H. F.; Bottero, J. Y.; Wiesner, M. R. Laboratory assessment of the mobility of nanomaterials in porous media. *Environ. Sci. Technol.* **2004**, *38* (19), 5164–5169.

(24) Wang, P.; Shi, Q. H.; Liang, H. J.; Steuerman, D. W.; Stucky, G. D.; Keller, A. A. Enhanced environmental mobility of carbon nanotubes in the presence of humic acid and their removal from aqueous solution. *Small* **2008**, *4* (12), 2166–2170.

(25) Liu, J.; Rinzler, A. G.; Dai, H. J.; Hafner, J. H.; Bradley, R. K.; Boul, P. J.; Lu, A.; Iverson, T.; Shelimov, K.; Huffman, C. B.; Rodriguez-Macias, F.; Shon, Y. S.; Lee, T. R.; Colbert, D. T.; Smalley, R. E. Fullerene pipes. *Science* **1998**, *280* (5367), 1253–1256.

(26) Petersen, E. J.; Akkanen, J.; Kukkonen, J. V. K.; Weber, W. J., Jr. Biological uptake and depuration of carbon nanotubes by *Daphnia magna*. *Env. Sci. & Tech.* **2009**, *43* (8), 2969–2975.

(27) Zhang, L.; Petersen, E. J.; Huang, Q. G. Phase distribution of 14C-labeled multi-walled carbon nanotubes in aqueous systems containing model solids: Peat. *Environ. Sci. Technol.* **2011**, *45* (4), 1356–1362.

(28) Petersen, E. J.; Nelson, B. C. Mechanisms and measurements of nanomaterial-induced oxidative damage to DNA. *Anal. Bioanal. Chem.* **2010**, *398* (2), 613–650.

(29) Warheit, D. B. How meaningful are the results of nanotoxicity studies in the absence of adequate material characterization? *Toxicol Sci.* **2008**, *101* (2), 183–185.

(30) Park, H.; Grassian, V. H. Commercially manufactured engineered nanomaterials for environmental and health studies: Important Insights provided by independent characterization. *Environ. Toxicol. Chem.* **2010**, *29* (3), 715–721.

(31) Bradford, S. A.; Torkzaban, S.; Walker, S. L. Coupling of physical and chemical mechanisms of colloid straining in saturated porous media. *Water Res.* **2007**, *41* (13), 3012–3024.

(32) Bradford, S. A.; Simunek, J.; Bettahar, M.; van Genuchten, M. T.; Yates, S. R., Significance of straining in colloid deposition: Evidence and implications. *Water Resour Res* **2006**, *42*, (12), W12S15.

(33) Elimelech, M.; Gregory, J.; Jia, X.; Williams, R. A., *Particle Deposition and Aggregation: Measurement, Modeling, and Simulation*; Butterworth-Heinemann: Oxford, 1995; p 441.

(34) Ko, C. H.; Bhattacharjee, S.; Elimelech, M. Coupled influence of colloidal and hydrodynamic interactions on the RSA dynamic blocking function for particle deposition onto packed spherical collectors. *J. Colloid Interface Sci.* **2000**, *229* (2), 554–567.

(35) Kuhnen, F.; Barmettler, K.; Bhattacharjee, S.; Elimelech, M.; Kretzschmar, R. Transport of iron oxide colloids in packed quartz sand media: Monolayer and multilayer deposition. *J. Colloid Interface Sci.* **2000**, *231* (1), 32–41.

(36) Kretzschmar, R.; Robarge, W. P.; Amoozegar, A. Influence of natural organic-matter on colloid transport through saprolite. *Water Resour. Res.* **1995**, *31* (3), 435–445.

(37) Tufenkji, N.; Elimelech, M. Spatial distributions of Cryptosporidium oocysts in porous media: Evidence for dual mode deposition. *Environ. Sci. Technol.* **2005**, *39* (10), 3620–3629.

(38) Johnson, P. R.; Elimelech, M. Dynamics of colloid deposition in porous-media—Blocking based on random sequential adsorption. *Langmuir* **1995**, *11* (3), 801–812.

(39) Tong, M. P.; Johnson, W. P. Excess colloid retention in porous media as a function of colloid size, fluid velocity, and grain angularity. *Environ. Sci. Technol.* **2006**, *40* (24), 7725–7731.

(40) Johnson, W. P.; Tong, M. P. Observed and simulated fluid drag effects on colloid deposition in the presence of an energy barrier in an impinging jet system. *Environ. Sci. Technol.* **2006**, *40* (16), 5015–5021.

(41) Li, X. Q.; Zhang, P. F.; Lin, C. L.; Johnson, W. P. Role of hydrodynamic drag on microsphere deposition and re-entrainment in porous media under unfavorable conditions. *Environ. Sci. Technol.* **2005**, *39* (11), 4012–4020.

(42) Tufenkji, N.; Elimelech, M. Correlation equation for predicting single-collector efficiency in physicochemical filtration in saturated porous media. *Environ. Sci. Technol.* **2004**, *38* (2), 529–536.